Mechanism of Carotenoid Singlet Excited State Energy Transfer in Modified Bacterial Reaction Centers

Su Lin,*,† Evaldas Katilius,† Robielyn P. Ilagan,‡ George N. Gibson,§ Harry A. Frank,‡ and Neal W. Woodbury†

Department of Chemistry & Biochemistry, Center for the Study of Early Events in Photosynthesis, and Biodesign Institute at ASU, Arizona State University, Tempe, Arizona 85287-1604, and Departments of Chemistry and Physics, University of Connecticut, Storrs, Connecticut 06269

Received: February 24, 2006; In Final Form: May 25, 2006

Ultrafast transient laser spectroscopy has been used to investigate carotenoid singlet excited state energy transfer in various *Rhodobacter (Rb.) sphaeroides* reaction centers (RCs) modified either genetically or chemically. The pathway and efficiency of energy transfer were examined as a function of the structures and energies of the donor and acceptor molecules. On the donor side, carotenoids with various extents of π-electron conjugation were examined. RCs studied include those from the anaerobically grown wild-type strain containing the carotenoid spheroidene, which has 10 conjugated carbon−carbon double bonds; the GA strain containing neurosporene, which has nine conjugated double bonds; and aerobically grown wild-type cells, as well as aerobically grown H(M182)L mutant, both containing the carbonyl-containing carotenoid spheroidenone, which has 11 conjugated double bonds. By varying the structure of the carotenoid, we observed the effect of altering the energies of the carotenoid excited states on the rate of energy transfer. Both S_1- and S_2-mediated carotenoid-to-bacteriochlorophyll energy transfer processes were observed. The highest transfer efficiency, from both the S_1 and S_2 states, was observed using the carotenoid with the shortest chain. The S_1-mediated carotenoid-to- bacteriochlorophyll energy transfer efficiencies were determined to be 96%, 84%, and 73% for neurosporene, spheroidene, and spheroidenone, respectively. The S_2-mediated energy transfer efficiencies follow the same trend but could not be determined quantitatively because of limitations in the time resolution of the instrumentation. The dependence of the energy transfer rate on the energetics of the energy transfer acceptor was verified by performing measurements with RCs from the H(M182)L mutant. In this mutant, the bacteriochlorophyll (denoted B_B) located between the carotenoid and the RC special pair (P) is replaced by a bacteriopheophytin (denoted ϕ_B), where the Q_X and Q_Y bands of ϕ_B are 1830 and 1290 cm^{-1}, respectively, higher in energy than those of B_B. These band shifts associated with ϕ_B in the H(M182)L mutant significantly alter the spectral overlap between the carotenoid and ϕ_B, resulting in a significant decrease of the transfer efficiency from the carotenoid S_1 state to ϕ_B. This leaves energy transfer from the carotenoid S_2 state to ϕ_B as the dominant channel. Largely because of this change in mechanism, the overall efficiency of energy transfer from the carotenoid to P decreases to less than 50% in this mutant. Because the spectral signature of ϕ_B is different from that of B_A in this mutant, we were able to demonstrate clearly that the carotenoid-to-P energy transfer is via ϕ_B. This finding supports the concept that, in wild-type RCs, the carotenoid-to-P energy transfer occurs through the cofactor located at the B_B position.

Introduction

The positions of the excited-state energy levels of carotenoids relative to those of chlorophylls (Chls) and bacteriochlorophylls (Bchls) determine their special roles in regulating the fate of excitation in photosynthetic systems through the dual functionality of light harvesting and photoprotection (for a review, see ref 1). Carotenoids absorb in the blue-green portion of the visible spectrum (420−550 nm), where Chls and Bchls have low extinction coefficients.[2] The study of singlet energy transfer from carotenoids to Chl or Bchl has been facilitated by the use of ultrafast laser spectroscopy (for a recent review, see ref 3) because of the nature of the short excited-state lifetimes of carotenoids.

Carotenoids can represent up to approximately 40% of the pigments in photosynthetic antenna systems and are found mostly in an all-trans configuration. A one-photon transition from the ground state (S_0) to the first excited singlet state (S_1) of carotenoids is optically forbidden because of symmetry. Carotenoid absorption bands in the visible region are due to a transition from the ground state to the second excited singlet state ($S_0 \rightarrow S_2$). In solution, the relaxation of S_2 to S_1 occurs in 50−300 fs,[4−6] depending on the carotenoid. The S_1 state lifetime of most of carotenoids in vitro varies from approximately 1 ps to hundreds of picoseconds.[1,7,8] The energy transfer efficiency from carotenoids to Chls or Bchls varies from 25 to ∼100%[9−11] and depends on the structure, geometry, location, and relative energy levels of the carotenoid and (B)chl molecules involved.

In anaerobically grown *Rb. sphaeroides*, a noncovalently bound spheroidene molecule is assembled in a 15,15′-cis configuration in the reaction center.[12−14] As shown in Figure 1,

* To whom correspondence should be addressed. E-mail: slin@asu.edu.
† Arizona State University.
‡ Department of Chemistry, University of Connecticut.
§ Department of Physics, University of Connecticut.

10.1021/jp061201d CCC: $33.50
Published on Web 07/18/2006

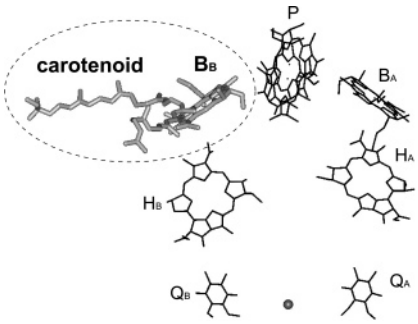

Figure 1. Arrangement of the cofactors of the wild-type photosynthetic reaction center from *Rb. sphaeroides* (from Protein Data Bank entry1AIJ). P, special pair composed of two strongly coupled bacteriochlorophyll *a* molecules; B_A and B_B, bacteriochlorophyll *a* monomers; H_A and H_B, bacteriopheophytins; Q_A and Q_B, ubiquinones. The pigments varied in the RCs are carotenoid and B_B, depicted in gray and circled. The WT RC contains spheroidene when grown under anaerobic conditions and spheroidenone when grown aerobically. The carotenoid is replaced by neurosporene in the GA-strain RCs. In the H(M182)L mutant, the bacteriochlorophyll *a* at the B_B position is replaced with a bacteriopheophytin *a*.

the RC consists of a set of cofactors arranged symmetrically to form two potential electron-transfer pathways (A and B branches). The cofactors include a pair of strongly coupled Bchl *a* molecules comprising the primary electron donor (P), two Bchl *a* monomers (B_A and B_B), two bacteriopheophytins (Bpheo, H_A, and H_B), and two quinones (Q_A and Q_B). The carotenoid is in proximity to B_B. The singlet excitation energy transfer efficiency from the carotenoid to the primary donor, P, has been reported to be ~75%, determined by steady-state fluorescence and time-resolved transient spectroscopy.[15,16] It has been postulated that singlet energy transfer from the carotenoid to P is mediated by B_B,[17,18] although direct evidence for a B_B intermediate excited state has not been resolved in the transient spectroscopic measurements.[16] The transient spectroscopic study also suggests that the cis configuration of the carotenoid in reaction centers, which is different from the all-trans configuration of carotenoids in many purple bacterial antenna proteins, is not a key factor in determining the efficiency of carotenoid-to-Bchl singlet excitation energy transfer. The fact that there is only one carotenoid predominately connected to B_B in the purple bacterial reaction center makes the system ideal for investigating the key factors that govern energy transfer from the carotenoid to Bchl.

Energy transfer can occur from both the S_1 and S_2 states of carotenoids to nearby Bchls. The length of the conjugated double-bond system in the carotenoid determines the extent of spectral and electronic orbital overlap with the acceptor (B)chl. The energy of the S_2 state in carotenoids, ranging from 21500 to 19000 cm^{-1} for carotenoids with 9−13 double bonds, is higher than that of the acceptor state of Bchl calculated from the Q_X transition at 600 nm to be 16670 cm^{-1}.[19−24] However, the S_2 lifetimes of carotenoids are short, in the range of 50−300 fs in solution, and therefore, the efficiency of excitation energy transfer from the carotenoid S_2 state is largely determined by the competition between the dynamics of relaxation and energy transfer. Carotenoid singlet excitation energy transfer can also occur from the S_1 state with more than 90% transfer efficiency.[5,9,11,25] The energy of the S_1 transition of carotenoids has been implicated as a key factor in controlling the overall efficiency of singlet-state energy transfer.[26−29]

To further understand the mechanism of carotenoid singlet energy transfer in photosynthetic systems, we studied carotenoid-to-P energy transfer in wild type, chemically modified, and mutant RCs. Both donor and acceptor molecular structures and excited-state energies were systematically varied to determine the factors controlling the efficiency of carotenoid-to-P energy transfer.

Materials and Methods

Procedures for the preparation of RCs of *Rb. sphaeroides* have been described previously.[30,31] Cells were grown either anaerobically in the light or aerobically in the dark. Under aerobic growth conditions, the majority of the reaction centers contain spheroidenone.[32−34] Under anaerobic growth conditions, the majority of the reaction centers contain spheroidene. Reaction centers were suspended in a buffer solution of 50 mM Tris-HCl (pH 8.0), 0.025% LDAO, 1 mM EDTA, and 0.1 mM *ortho*-phenanthroline. An optical density of roughly 1 in a spinning sample wheel at 802 nm was used. All measurements were performed at room temperature.

The femtosecond transient absorption spectrometer at Arizona State University that was used in this study has been described previously.[16] Laser pulses of 100 fs at 790 nm were generated from an amplified, mode-locked titanium sapphire kilohertz laser system (CPA-1000, Clark-MXR). Part of the laser pulse energy (~15%) was used to generate a white-light continuum for the probe beams (sample and reference). The remainder of the pulse energy was used to pump a modified optical parametric amplifier (IR-OPA, Clark-MXR) to generate excitation pulses at 490 nm. The excitation intensity was adjusted using a continuously variable neutral-density filter. Transient absorption changes were measured over two spectral ranges from 460 to 760 nm and from 730 to 1030 nm using a dual diode array detector (DPDA, Princeton Instruments). The relative polarization of the excitation and probe beams was set at the magic angle. Time-resolved spectra were recorded every 91 fs with a spectral resolution of 2 nm. The energy per pulse was kept below 2 μJ with a spot size of 1-mm diameter to avoid multiphoton excitation of the reaction centers. The integrity of the sample was checked before and after the experiment by absorption spectroscopy.

Time-resolved spectra were corrected for spectral dispersion.[16] Data analysis was carried out using locally written software (ASUFIT) developed under a MatLab environment.

Results

Ground-State Absorption of the Reaction-Center Carotenoid. Ground-state absorption spectra of reaction centers from anaerobically grown wild-type (WT) *Rb. sphaeroides*, the GA mutant strain, aerobically grown WT, and the H(M182)L mutant were recorded at 298 K (Figure 2). The GA mutant contains neurosporene (actually a mixture of neurosporene, hydroxyneurosporene, and methoxyneurosporene, in the ratio 48:37:14), which has 9 conjugated carbon−carbon double bonds ($N = 9$).[35] Anaerobically grown WT RCs contain spheroidene, which has 10 conjugated double bonds ($N = 10$). Both WT and the H(M182)L mutant grown under aerobic conditions contain spheroidenone with 11 conjugated double bonds ($N = 11$). The RC absorption spectra containing different carotenoids show very similar spectral features in the Bchl and Bpheo absorption regions, except for the H(M182)L mutant. In the H(M182)L mutant, changing the histidine ligand to leucine at the position H(M182)L results in the replacement of the Bchl by a Bpheo (this pigment is referred to as ϕ_B; see ref 30). The corresponding spectral changes include a blue shift of the 802-nm band to 797 nm, a decrease of the oscillator strength of the Q_X band at 600 nm, and an increase in the absorbance of the Bpheo Q_X band at 540 nm.

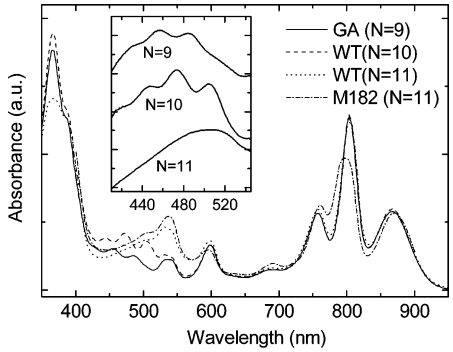

Figure 2. Absorption spectra of RCs from the GA strain containing neurosporene (solid line), WT containing spheroidene (dashed line), WT containing spheroidenone (short dashed line), and the H(M182)L mutant (dotted-dashed line) containing spheroidenone. The GA and two WT curves are normalized at their 800-nm peaks. The absorption spectrum of the H(M182)L mutant was normalized to the WT spectrum on the longer-wavelength side of the 860-nm band. The inset shows difference spectra representing absorption of various carotenoids, neurosporene (upper curve), spheroidene (middle curve), and spheroidenone (lower curve). The curves in the inset were obtained by subtracting the absorption spectrum of carotenoid-less R26 RC from the corresponding carotenoid-containing absorption spectra.

Spectral variations due to the different carotenoids are seen in the wavelength region between 420 and 580 nm. Carotenoids containing 9 or 10 double bonds absorb between 420 and 520 nm, whereas spheroidenone has its absorption in the 480−580-nm region. The absorption spectra of the three different carotenoids in the absence of the other pigments (inset, Figure 2) were estimated by subtracting the absorption spectrum of carotenoid-less RCs (*Rb. sphaeroides* strain R-26) from those containing neurosporene, spheroidene, or spheroidenone. The structure of the vibronic bands can be seen clearly for carotenoids with $N = 9$ and 10. The vibrational band structure is diminished in the case of spheroidenone ($N = 11$), likely because of the additional carbonyl group presents in a polar environment.[36] Previous studies of carotenoids in solution have shown that the energies of the carotenoid S_0-to-S_2 transition vary with the number of conjugated double bonds.[23,24,37] The longer the carotenoid chain, the lower the energy of the S_2 transition. The same trend applies to the S_1 energy level, but the effect is larger. The changes in the carotenoid S_2 absorption bands as a function of the number of conjugated double bonds in the RC (Figure 2, inset) agree very well with those observed in solution.[5,7,38] The two carotenoids with $N = 9$ and 10 absorb at shorter wavelengths than the carotenoid in aerobically grown WT and the H(M182)L mutant, both of which contain spheroidenone with $N = 11$. The latter two RCs show similar absorption spectral profiles except that the H(M182)L mutant has a higher absorption peak at 540 nm due to the absorption of the additional Bpheo (ϕ_B).

Carotenoid Excitation Energy Transfer in Spheroidenone-Containing RCs. Transient absorption changes of aerobically grown WT ($N = 11$) and H(M182)L mutant ($N = 11$) RCs were recorded between 450 and 700 nm at room temperature. Excitation at 490 nm was used for these studies, preferentially exciting the carotenoid S_0-to-S_2 transition. The time-resolved spectra recorded at different time delays are compared in Figure 3. At the earliest time shown, the absorbance change spectrum in this wavelength region is dominated by carotenoid excited states. Spectral changes at 0.5 ps show a broad bleaching centered around 500 nm and an absorption increase above 540 nm. The initial bleaching at 500 nm is due to the formation of the carotenoid S_2 excited state resulting from direct excitation

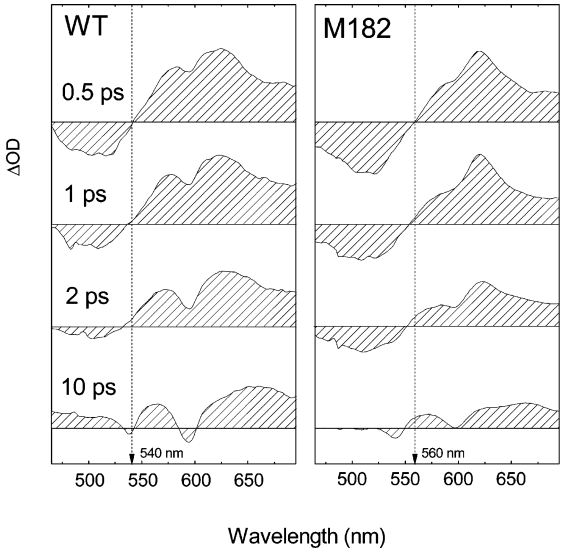

Figure 3. Comparison of time-resolved spectra of WT and H(M182)L RCs in the carotenoid and bacteriopheophytin/bacteriochlorophyll Q_X transition region at 0.5, 1, 2, and 10 ps. The vertical scales for time-resolved spectra from one sample are kept the same. The vertical scales for different sets of spectra are scaled in such a way that signals for the carotenoid $S_1 \rightarrow S_N$ transition at 0.5 ps are about the same size. The vertical dashed lines positioned at the zero cross of the time-resolved spectra recorded at 0.5 ps are at 540 and 560 nm for WT and the H(M182)L mutant, respectively.

of the carotenoid S_0-to-S_2 transition band. The positive band above 540 nm is due to the carotenoid S_1-to-S_N transition which reaches its maximum 200−300 fs after excitation of S_2, as previously observed for WT ($N = 11$).[16] Spectral changes at 1, 2, and 10 ps show the decay of the carotenoid excited states and the formation of the primary charge-separated state $P^+H_A^-$ [or $P^+H_A^- + P^+\phi_B^-$ in the H(M182)L mutant, as described previously[30]]. Several differences were observed between the absorbance change spectra of aerobically grown WT RCs and those of the H(M182)L mutant. A bleaching at 595 nm superimposed on the carotenoid excited-state absorption band is apparent in the 0.5-ps spectrum for both samples, but the size of the bleaching signal varies. This band is due to the ground-state bleaching of P or B. In the early-time spectra (0.5 and 1 ps), the amplitude of the 595-nm bleaching band is much stronger in WT RCs than in the H(M182)L mutant. The simultaneous decay of the negative and positive signals due to carotenoid excited states and the development of the 595-nm bleaching associated with charge separation were observed in the time-resolved spectra taken at later times in both RCs. For similar amounts of carotenoid S_1 excited state formed, judging from the amplitude of the positive signal between 550 and 650 nm at 0.5 ps, the total yield of the charge-separated states $P^+H_A^- + P^+\phi_B^-$ for the H(M182)L mutant is lower than that of $P^+H_A^-$ formed in WT RCs. In addition, there is a 20-nm red shift of the zero crossing wavelength in the mutant compared to the WT at 0.5 ps (marked by the vertical lines in Figure 3). The bleaching band below 550 nm observed for H(M182)L RCs is broader and red-shifted relative to that for WT. This is due to bleaching of the Bpheo around 540 nm in the H(M182)L mutant, implying that the excitation from the carotenoid is predominately transferred to ϕ_B. All of these changes are observed within the first few hundred femtoseconds in the mutant, suggesting that they are due to excitation energy transfer from the carotenoid S_2 state to the Q_X state of ϕ_B. The spectral differences at 10 ps indicate that the final yield of the total charge-separated state ($P^+H_A^- + P^+\phi_B^-$) formed in H(M182)L is about 30−40% of

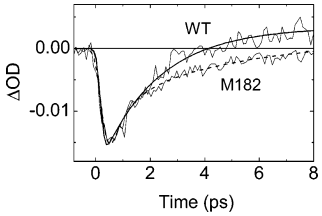

Figure 4. Comparison of carotenoid ground-state recovery kinetics at 500 nm for WT and the H(M182)L mutant, both of which contain spheroidenone ($N = 11$). Smooth lines are theoretical fitting curves. See text for details.

the yield of $P^+H_A^-$ formed in WT, judging from the amplitude of the 595-nm bleaching, which represents the amount of P^+ formed at 10 ps. For the comparison between H(M182)L and WT, the samples were normalized to have the same total S2 bleaching at early time.

Global exponential analysis of the transient data in the 470−700-nm region for the spheroidenone-containing WT and the H(M182)L mutant ($N = 11$) revealed three kinetic components at 100−300 fs, 2−5 ps, and 200 ps and a nondecaying component. The shortest-lived component represents the decay of the carotenoid S_2 excited state. This is on the order of the excitation pulse duration and probe spectral dispersion, and therefore, precise early-time kinetics cannot be accurately determined in this study. However, the ultrafast kinetic component is necessary in the global fitting, indicating the existence of this fast process. The 2−5-ps component represents a mixture of several kinetic processes, including the decay of the carotenoid S_1 state, the formation of excited states of B (or ϕ_B), and the formation of charge-separated state(s). The 200-ps and nondecaying components are related to the secondary electron-transfer processes.

Figure 4 compares kinetic traces of WT and H(M182)L RCs at 500 nm, the wavelength dominated by carotenoid signals. It can be seen that the carotenoid excited state recovers within 3 ps in WT RCs, whereas a slower recover time is clearly observed in the H(M182)L mutant; a substantial amount of the carotenoid does not recover until 8 ps. To extract the lifetimes representing the carotenoid S_1 and S_2 states more precisely, ground-state recovery kinetic measurements at 500 nm were fit at a single wavelength (Figure 4), which returned time constants of 0.2 ± 0.05 and 1.8 ± 0.2 ps for WT and 0.1 ± 0.05 and 5.6 ± 0.4 ps for H(M182)L (both $N = 11$), as well as a long-lived component with a low amplitude of a few percent of the total. The subpicosecond [0.2 ps for WT and 0.1 ps for the H(M182)L mutant] carotenoid excited-state recovery kinetics, together with the appearance of ground-state bleaching amplitudes of B and/or P (WT) or ϕ_B (M182 mutant) in the time-resolved spectra measured within 1 ps, clearly show that a very fast energy transfer occurs from the carotenoid to Bchl [or to ϕ_B in the H(M182)L mutant], which is most likely from the carotenoid S_2 state rather than S_1. The 1.8-ps component in WT is due to the decay of the carotenoid S_1 state, as observed previously.[16] The 5.6-ps decay lifetime that represents the excited-state lifetime of the carotenoid (spheroidenone) in the H(M182)L mutant is very similar to that found in solution.[36]

Excited-State Lifetimes of Carotenoids with Different Conjugation Lengths. To obtain a better understanding of how the transition energies of the donor carotenoid affects the pathway and efficiency of energy transfer, RCs containing carotenoids with different numbers of conjugated double bonds (neurosporene, $N = 9$; spheroidene, $N = 10$; and spheroidenone, $N = 11$) were studied. Kinetics at selected wavelengths where the difference absorbance spectrum is dominated by changes

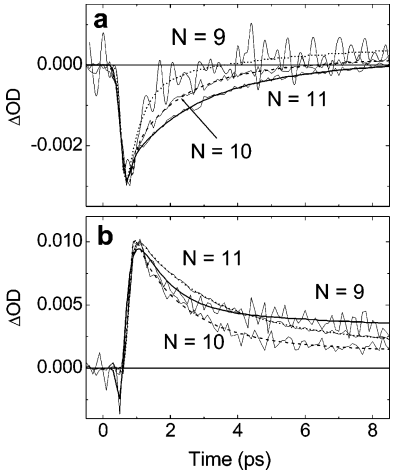

Figure 5. (a) Comparison of carotenoid ground-state bleaching kinetics of GA strain ($N = 9$), WT with spheroidene ($N = 10$), and WT with spheroidenone ($N = 11$). Kinetic traces were recorded at 470 nm for $N = 9$ and 10 and at 510 nm for $N = 11$ and were normalized at their bleaching maxima. (b) Kinetic traces measured at the carotenoid S_1-to-S_N transition wavelength at 570, 570, and 577 nm for $N = 9$, 10, and 11, respectively. Smooth lines in each panel are theoretical fitting curves ($N = 9$, short dashed lines; $N = 10$, dashed lines; $N = 11$, solid lines). See text for details.

in the carotenoid ground-state population and S_1 excited-state population are compared in Figure 5a,b, respectively. Kinetic traces of both the ground-state recovery (between 470 and 510 nm) and the S_1-to-S_N transition (between 570 and 625 nm) were fit to a series of exponential decay components. The fitting reveals four kinetic components in both wavelength regions for all three RC samples. A 100−200-fs component shows recovery of ground-state bleaching and buildup of the S_1-to-S_N signal. This component likely represents the carotenoid S_2 lifetime. Again, the variation of the fastest lifetime between the different carotenoids is difficult to interpret because of the limited instrument response, as are the large amplitudes of this component. The 1−2- and 3−5-ps components represent the carotenoid S_1 decay and the contributions from other RC cofactors due to the formation of the charge-separated states. The 200-ps decay is due to the secondary electron transfer from H_A to Q_A and makes only a minor contribution to the spectral changes in the 470−510-nm wavelength region. To obtain a more reliable carotenoid S_1 decay lifetime, the 3−5- and 200-ps lifetimes were held constant in the fit, and the fit was also performed using the data obtained after the excitation pulse was complete in order to deemphasize the ultrafast component in the fitting process. In summary, the analysis of the carotenoid kinetics resulted in S_1 lifetimes of 0.8 ± 0.2, 1.4 ± 0.1, and 1.6 ± 0.1 ps for RCs containing carotenoids with $N = 9$, 10, and 11 conjugated double bonds, respectively. The change in the S_1 lifetime as a function of the length of the carotenoid chain implies that the shorter the carotenoid chain, the faster the decay of its S_1 state. This observation agrees well with previous measurements from photosynthetic antenna systems.[27,29]

Spectral Changes and Kinetics on the Acceptor Side. Steady-state and transient absorption spectra in the Bchl Q_Y transition region between 730 and 980 nm from aerobically grown WT ($N = 11$) and the H(M182)L mutant are compared in Figure 6. The vertical dotted lines are set at the B_A/B_B absorption maximum wavelength of 802 nm. For the WT RC containing spheroidenone ($N = 11$), the initial absorbance changes are dominated by ground-state bleaching of the Bchl monomers around 802 nm. P-band bleaching develops on a subpicosecond time scale, and the spectral signature of $P^+H_A^-$

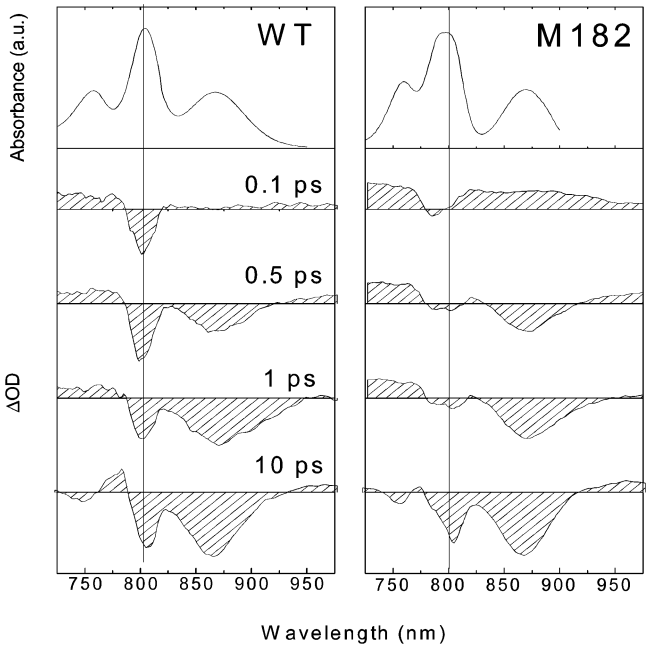

Figure 6. Steady-state absorption spectra (upper panels in each column) and time-resolved spectra of WT and H(M182)L RCs in the bacteriopheophytin and bacteriochlorophyll Q_Y transition region at 0.1, 0.5, 1, and 10 ps. The vertical scales for time-resolved spectra from the same sample are kept the same. Time-resolved spectra from different samples are scaled in such a way that their P-band bleaching signals at 10 ps have similar amplitudes. The vertical dotted lines are placed at 802 nm in all panels.

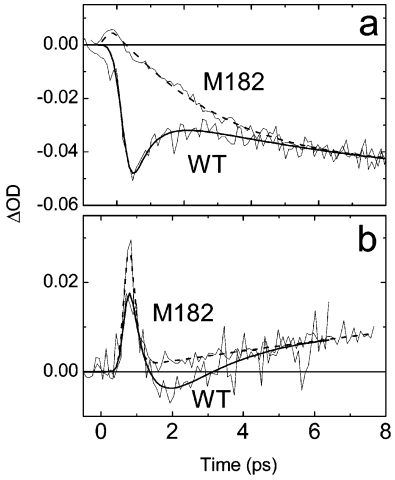

Figure 7. Kinetic traces of WT and H(M182)L at (a) 802 nm, the monomer Bchl *a* absorption wavelength and (b) 990 nm, the carotenoid excited-state absorption wavelength. The former reflects the kinetics of the ground-state bleaching or electrochromic shift of B_A/B_B in WT RC and B_A in the H(M182)L mutant, where the latter represents the kinetics of carotenoid excited state. The smooth lines are theoretical fittings obtained from global analysis in the Q_Y transition region from 740 to 990 nm, using three exponential decays and a nondecaying component [WT, solid line; H(M182)L mutant, dashed line]. See text for details.

is fully formed by 10 ps. The H(M182)L mutant contains a Bpheo at the B_B position, resulting in a blue shift of the monomer absorption bands. The time-resolved spectrum at 0.1 ps clearly shows that, after carotenoid excitation, the first absorption change observed in the Q_Y region involves a bleaching at 780 nm, corresponding to the ground-state absorption of ϕ_B. This band maintained a relatively small amplitude in comparison to the B-band bleaching in WT RCs, and its recovery was accompanied by the growth of the P-band bleaching. There is a time delay in the development of the absorbance decrease near 802 nm in the H(M182)L mutant.

Although the kinetics in this wavelength region is complex, it can be fit to a reasonable approximation with three exponential decay terms and a nondecaying component over the wavelength region from 740 to 980 nm globally, providing a means of comparing the spectral and kinetic changes for aerobically grown WT ($N = 11$) and H(M182)L. The subpicosecond component, 0.2−0.5 ps, represents an overall excitation transfer from carotenoid to P, most likely via B_B [ϕ_B in the H(M182)L mutant]. The 3−5-ps component is dominated by the formation of charge-separated states. The 200-ps decay component is due to the secondary electron transfer. Finally, the nondecaying component represents the long-lived secondary charge-separated state(s). The kinetic traces recorded at 802 nm from WT ($N = 11$) and the H(M182)L mutant are shown in Figure 7a, with signals normalized at 10 ps. The signal mostly represents the spectral changes associated with the B_A and/or B_B ground states. Rapid formation of an 802-nm absorbance decrease was observed in WT ($N = 11$) RCs, followed by at least partial recovery of this decrease within 1 ps, presumably because of a rapid buildup of the excited state of B due to ultrafast energy transfer from the carotenoid S_2 state to B, followed by energy transfer from B to P. In contrast, no initial bleaching is observed in the H(M182)L mutant. The appearance of the 802-nm bleaching takes up to several picoseconds, most likely because, in the H(M182)L mutant, this represents formation of $P^+H_A^-$ and the associated electrochromic shift of the B_A ground-state band. Apparently, there is no direct excitation energy transfer from the carotenoid to the Bchl monomer on the A side.

The energy transfer pathway of carotenoid → ϕ_B → P is certainly the simplest interpretation of the time-resolved spectra of the H(M182)L mutant. Judging from the results for the H(M182)L mutant, it is very likely that, in WT, only the Bchl on the B side is involved in the carotenoid-to-P transfer, and this is certainly what one would expect from the positions of the cofactors involved.

It is worth noting that a broad absorption increase is observed over the entire Q_Y wavelength region shortly after time zero in both RCs studied, which decays with a lifetime of less than 1 ps. This broad absorption increase appears more intensely in the H(M182)L mutant than in WT RCs. It is possible that, in the H(M182)L mutant, the relatively low ϕ_B and P bleaching at early times in this region makes the positive-going signal appear more pronounced. The characteristic kinetics of this signal at 990 nm from WT ($n = 11$) and the H(M182)L mutant are plotted in Figure 7b. Signals are normalized to the amplitudes observed at times longer than 10 ps. This prompt absorbance increase in the near-infrared region is likely associated with carotenoid excited states, judging from their spectral profiles and lifetimes. This is discussed in more detail below. Similar spectral changes have been observed previously.[39,40]

Discussion

Recent structural studies in conjunction with ultrafast laser spectroscopic studies have greatly extended our knowledge of excited-state properties of carotenoids. For example, the 2-Å resolution structure of LH2 shows that the carotenoid is in close contact with both the B800 and B850 Bchls.[41,42] In this structure, the carotenoid is located between 5.4 and 9.3 Å from the center of the Bchls. This kind of arrangement in LH2 allows carotenoids to serve as efficient energy donors in the light-harvesting process. However, a large variation of carotenoid singlet

excitation energy transfer efficiencies, ranging from 25% to nearly 100%, has been found in LH1 and LH2 from different species. One of the key factors that directly affects the transfer efficiency is the number of conjugated double bonds in the carotenoid. For similar geometric pigment arrangements and protein environments, a carotenoid with a longer conjugated bond system will have lower transfer efficiency than one with a shorter conjugated network. Studies have shown that, in LH2 of purple bacteria, the number of double bonds (N) determines the carotenoid S_2 and S_1 excited-state energy levels and their lifetimes and therefore controls the carotenoid-to-Bchl energy-transfer rates and pathways and thus the overall efficiency.[5,9,11,25−27,43−47] In this work, we varied the structure, and therefore the energy levels, of both the carotenoid donor and the Bchl acceptor to study the mechanism and pathway of singlet energy transfer from the carotenoid to P in the reaction center. Past work has shown that, for carotenoids with $N = 9-11$, the S_2 energy varies from 21300 cm^{-1} (469 nm) to 19500 cm^{-1} (513 nm), and the energy of S_1 varies from 15300 cm^{-1} (654 nm) to 13000 cm^{-1} (765 nm).[20,26,29,36,48−50] For a carotenoid with N=11, varying the acceptor energy from Bchl (B_B) at 12500 cm^{-1} (800 nm) to Bpheo (ϕ_B) at 13000 cm^{-1} (767 nm) made it possible to identify the pathway and explore the mechanism of carotenoid-to-P energy transfer in some detail.

Carotenoid-to-P Energy Transfer Pathways. Previous ultrafast spectroscopic studies have shown that the excited-state energy of the RC carotenoid is transferred efficiently to P via B.[16] The energy transfer pathway was inferred from the fact that the 800-nm bleaching (monomer Bchl) appears prior to bleaching of the P band near 860 nm. Whether the 800-nm bleaching is actually associated with the monomer on the A or B side could not be resolved because of spectral overlap. It was simply assumed that, because B_B is structurally situated between P and the carotenoid, this bacteriochlorophyll served as the energy transfer intermediate. In the current study, a careful comparison of early-time spectral evolution was carried out using both WT ($N = 11$) and the H(M182)L mutant (also $N = 11$) reaction centers. In the H(M182)L mutant, the spectral overlap between the molecules in the carotenoid-to-P energy-transfer chain is shifted dramatically compared to that in wild type because Bchl at the B_B position is replaced by Bpheo. Figures 3 and 5 show that, upon excitation of carotenoid to its S_2 state, the B-band bleachings at 595 and 800 nm appear on subpicosecond time scales in RCs with Bchl as the energy acceptor whereas the dominant ultrafast bleaching observed in the H(M182)L mutant are at 540 and 785 nm, the wavelengths of ϕ_B absorption. In the H(M182)L mutant, the decrease in absorbance at 800 and 860 nm appears a few hundred femtoseconds later, presumably because of further energy transfer from ϕ_B to P, followed by the formation of $P^+\phi_B^-$ and $P^+H_A^-$, as observed previously.[30] As mentioned in the Results section, the overall bleaching of ϕ_B at 780 nm is weaker than that observed for B_B bleaching at 802 nm in WT ($N = 11$). This is probably due to the weaker oscillation strength of ϕ_B rather than the slower energy transfer from carotenoid to ϕ_B or faster transfer from ϕ_B to P. The fact that Bpheo bleaching in the Q_Y region is weaker than that of the B band bleaching was observed in WT under similar excitation conditions in the past, even with direct excitation (see ref 51, for example). The kinetics of the H(M182)L mutant in the B_A absorption region around 800 nm shows no sign of early B-band bleaching within the first picosecond (Figure 7a). The observation that ϕ_B receives excitation prior to B_A in the H(M182)L mutant supports the conclusion that the energy transfer from carotenoid to P is via the cofactor located between carotenoid and P on the B side, consistent with previous conclusions based on the location of the carotenoid molecule in RCs.[17] Thus, in the H(M182)L mutant, the energy-transfer pathway can be directly identified as ^{1}carotenoid $\rightarrow$ $^1\phi_B \rightarrow {}^1$P, and the location of B_B in close proximity to the carotenoid (5−6 Å) and P (10 Å) makes it the only candidate for bridging the transfer in the wild-type RC as well.

Carotenoid S_2-Mediated Energy Transfer. On the basis of studies of carotenoid-to-Bchl energy transfer in a large number of light-harvesting systems, it has been concluded that both the carotenoid S_1 and S_2 states can be actively involved. Moreover, the transfer pathways and efficiencies are governed mainly by the conjugation length of the carotenoid. Considering the relative energy levels of the carotenoid and Bchls, it is most likely that the energy from the carotenoid S_2 state is transferred to the Bchl Q_X state whereas the energy from the carotenoid S_1 state is transferred to the Bchl Q_Y state. In principle, both the S_2- and S_1-mediated transfer efficiencies can be obtained by comparing their lifetimes in solution and in vivo, assuming that the carotenoid intrinsic lifetimes are not altered substantially in the protein environment.[52] The S_2 lifetime could not be determined accurately from the measurements reported here because it is within the time duration of the excitation pulse width, and the dispersion artifact in pump−probe spectroscopy makes an accurate deconvolution on this time scale difficult. However, inspection of the kinetics of carotenoid ground-state bleaching in Figure 5a reveals a clear trend. The ratio of the amplitudes of the fast and slow components, dominated by the carotenoid S_2 and S_1 decay kinetics, varies with the type of carotenoid in the RC. The shorter the carotenoid chain, the larger the ratio (i.e., greater contribution from the fast component). This provides a general idea about the S_2-to-Bchl energy transfer efficiency in various RCs. In previous work, it was determined that 30% of the total amplitude of the B bleaching at 595 nm appeared on subpicosecond time scales in WT RCs ($N = 11$).[16] This was attributed to either direct excitation of Bchl (B or P) or fast carotenoid-to-Bchl transfer. The fast carotenoid ground-state recovery kinetics expected for energy transfer was not clearly observed, but given the time resolution of the instrument and the relatively small fraction of the signal (30%) that was expected to decay rapidly, it was not possible to arrive at an unambiguous conclusion. However, in the case of the reaction centers containing $N = 9$ and 10 carotenoids used in the current study, the subpicosecond decay component is seen more clearly. This suggests that the fast recovery phase of the Bchl ground-state bleaching is due to carotenoid-to-Bchl energy transfer from the S_2 excited state of the carotenoid, rather than the direct excitation of B. The carotenoid S_2-to-Bchl transfer efficiency is expected to be higher than 30% for shorter chain carotenoids, judging from observations of bacterial light-harvesting systems.[5,9,11,25−27,43−47]

In the H(M182)L mutant, the occurrence of efficient excitation energy transfer from the carotenoid S_2 excited state to ϕ_B was concluded on the basis of the observation that the ϕ_B Q_X bleaching around 545 nm appears on the subpicosecond time scale. The overall carotenoid-to-P energy transfer in the H(M182)L mutant is discussed later.

Carotenoid S_1-Mediated Energy Transfer. Energy from the carotenoid S_1 state likely transfers into the Bchl Q_Y state. Compared to the S_2 excited state, the S_1 lifetime is much longer, on the order of picoseconds to even hundreds of picoseconds.[1,7,8] An important parameter that governs the transfer efficiency is the position of the S_1 energy level. Past studies have also shown that, for carotenoids without the carbonyl group, both the

lifetime and energy of the S_1 state are insensitive to the solvent polarity and temperature.[52] This has also been found to be true in the case of spheroidenone, even though it contains the carbonyl group.[36,52] Thus, it should be possible to estimate accurately the S_1-mediated energy transfer efficiency in pigment−protein complexes by comparison of the S_1 lifetime in the RC to that in solvent. Analysis of the absorbance changes in the carotenoid excited state spectral region revealed S_1 lifetimes of 0.8 ± 0.2, 1.4 ± 0.1, and 1.6 ± 0.1 ps for RCs containing carotenoids with $N = 9$, 10, and 11, respectively. Using their S_1 lifetimes of 24, 8.5, and 6 ps measured in solution,[20,36,53] efficiencies of the carotenoid S_1-to-B_B transfer were determined to be 96%, 84%, and 73%, respectively. The dependence of S_1-mediated energy transfer efficiency on the carotenoid conjugation length in RCs in this study can be compared with that observed in the LH2 antenna system from purple bacteria by several groups using similar time-resolved spectroscopic techniques.[27,29,43] In the study of Desamero et al., a series of spheroidene analogues incorporated in the B850 light-harvesting complex with *N* ranging from 7 to 13 were examined. An energy transfer efficiency of 52% was concluded for transfer from spheroidene ($N = 10$) to the B850 chls. In Zhang et al.'s study, neurosporene ($N = 9$), spheroidene ($N = 10$), and lycopene ($N = 11$) were incorporated into LH2 to investigate the S_1-mediated energy transfer, and efficiencies of 94%, 82%, and 30%, respectively, were obtained. A recent study by Polivka et al. showed transfer efficiencies of 94%, 82%, and 76%, respectively, for neurosporene ($N = 9$), spheroidene ($N = 10$), and spheroidenone ($N = 11$) incorporated into LH2. Our results are in excellent agreement with those in Polivka et al.'s work, which used the same group of carotenoids. The results are also in good agreement with Zhang et al.'s work for $N = 9$ and 10, but they show a significant discrepancy for $N = 11$. This could be due to the presence of the carbonyl group in spheroidenone, which is not present in the lycopene used in Zhang et al.'s study. The presence of a C═O group in spheroidenone makes the conjugated double bond of spheroidenone effectively shorter than that of lycopene. As a consequence, the S_1 energy of spheroidenone is higher than that of lycopene, which could be responsible for the higher carotenoid-to-Bchl energy transfer efficiency.[36,43,52]

In the H(M182)L mutant, the slow phase of the carotenoid excited state recovery resembles that of the spheroidenone in solution, suggesting that the amount of energy transfer from the S_1 state to the Bpheo in this mutant is much less than the carotenoid to Bchl energy transfer efficiency in WT RCs. Thus, in the H(M182)L mutant, the dominant carotenoid-to-ϕ_B transfer pathway is from the S_2 state. The overall transfer efficiency from carotenoid to P in this mutant is 30−40%, as determined by comparing the P^+ yield of the H(M182)L mutant with that of WT when the two data sets are normalized such that they show equal amounts of initially generated carotenoid excited state. The previous study by King et al. showed that the energy-transfer kinetics from ϕ_B to P in the H(M182)L mutant is very similar to that from B_B to P in the WT RCs;[54] therefore, a similar yield of P^+ formation is expected. The lower P^+ yield of the H(M182)L mutant compared to that of WT observed in this study is likely due to the diminished energy transfer from the carotenoid S_1 state to ϕ_B. It is not difficult to understand why the carotenoid S_1-to-ϕ_B energy transfer efficiency is low in the mutant. The S_1 state energy from spheroidenone was estimated to be approximately 13000 cm^{-1} (769 nm) from the measurements of the S_1-S_2 spectral profile in solution.[36] It has been shown in recent studies that, for carotenoids with a carbonyl group, a combined S_1/ICT state can be formed in polar solvent with an energy lower than that of the S_1 state.[36] This S_1/ICT state was found to quench the excited-state energy of a nearby molecule Bchl *a* molecule.[55] As the energy of the ϕ_B Q_Y transition is 12740 cm^{-1} (785 nm), a similar quenching mechanism could by responsible for the poor spheroidenone S_1-to-ϕ_B Q_Y energy transfer observed in this study.

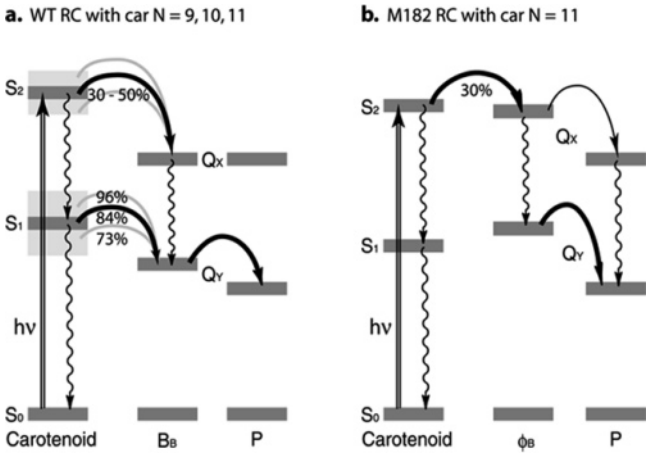

Figure 8. Energy diagram and proposed kinetic model for carotenoid-to-P singlet excited state energy transfer in (a) WT RCs and (b) the H(M182)L mutant RCs in which Bchl (B_B) is replaced by Bpheo (ϕ_B). Light gray boxes near the carotenoid S_1 and S_2 energy levels in a illustrate the range of energy changes due to the variation of the carotenoid. Arrows represent energy transfer pathways, and numbers indicate the transfer efficiencies obtained from this study.

Overall Carotenoid-to-P Energy Transfer. Previous studies have shown that the excitation energy transfer from B to P occurs on the 100-fs time scale. Although the spectral overlap between ϕ_B and P is significantly different from that between B_B and P, selective excitation studies of the ϕ_B mutant still show an ultrafast energy transfer from ϕ_B to P that cannot be distinguished from the transfer efficiency of the wild type.[54,56] This could be due to close contact between the donor and acceptor, resulting in strong electronic coupling or a partial electronic orbital overlap.

If the final energy transfer step to P is not rate-limiting in either the wild type or H(M182)L mutant, then the overall carotenoid-to-P energy transfer rate (and presumably the efficiency) must be governed by the transfer from the carotenoid to B_B (or ϕ_B). A proposed energy diagram showing the positions of the various carotenoid excited states relative to those of B_B (or ϕ_B) and P in *Rb. sphaeroides* RCs is shown in Figure 8. The light gray boxes superimposed on the carotenoid S_1 and S_2 energy levels illustrate the energy variations of the different carotenoids studied. Various transfer pathways are proposed in accordance with the experimental results. Excitation of carotenoid around 500 nm results in the carotenoid S_0-to-S_2 transition, followed by relaxation of the excited state to S_1 within a few hundred femtoseconds. Part of the excitation energy of S_2 is transferred to the Bchl through the Q_X state; the efficiency is dependent on the relative energies of the donor and acceptor states as illustrated in Figure 8a. The excitation energy in the carotenoid S_1 state is transferred to the Bchl through the Q_Y states on a picosecond time scale, again depending on the relative energy levels of the donor and acceptor. Energy transfer from both the carotenoid S_2 and S_1 states was observed for all carotenoids studied, but the efficiency varied with conjugated chain length. The S_1-mediated transfer efficiencies were determined to be 96%, 84%, and 73% for the carotenoids with 9, 10, and 11 conjugated double bonds, respectively. The caro-

tenoid S_2-mediated transfer seems also to follow the same trend but could not determined precisely.

The H(M182)L mutant has a substantial effect on the carotenoid-to-P energy transfer rate and efficiency, judging from the low yield of the total charge-separated state ($P^+H_A^-$ + $P^+\phi_B^-$). On the basis of the facts that energy transfer from the carotenoid S_2 state to ϕ_B is observed at early times and the amount of further development of P^+ signal does not match the amount of decay of the carotenoid S_1 stated decay, it is concluded that the lower yield of P^+ formation in the mutant is mostly due to the lack of energy transfer from the carotenoid S_1 state to the nearby Bpheo (ϕ_B), as shown in Figure 8b. Another possibility is that the excitation energy of ϕ_B generated from both the carotenoid S_2 and S_1 excited states is transferred back to the carotenoid. This can also explain the relatively high absorption increase observed in the 730−970-nm wavelength region from the H(M182)L mutant. In this mutant, more carotenoid S_1 excited state and less P bleaching are present at any time, resulting in a more intense carotenoid excited-state absorption signal.

Acknowledgment. This work was supported at ASU by the National Science Foundation (MCB-0131776) and at the University of Connecticut by a grant from the National Institutes of Health (GM-30353). This is publication #667 from the Center for the Study of Early Events in Photosynthesis, Arizona State University.

References and Notes

(1) Frank, H. A.; Cogdell, R. J. In *Carotenoids in Photosynthesis*; Young, A. J., Britton, G., Eds.; Chapman & Hall: London, 1993; pp 252−326.

(2) Koyama, Y.; Kuki, M.; Andersson, P. O.; Gillbro, T. *Photochem. Photobiol.* **1996**, *63*, 243−256.

(3) Polivka, T.; Sundstrom, V. *Chem. Rev.* **2004**, *104*, 2021−2071.

(4) Macpherson, A. N.; Gillbro, T. *J. Phys. Chem. A* **1998**, *102*, 1089−5639.

(5) Ricci, M.; Bradforth, S. E.; Jimenez, R.; Fleming, G. R. *Chem. Phys. Lett.* **1996**, *259*, 381−390.

(6) Akimoto, S.; Yamazaki, I.; Takaichi, S.; Mimuro, M. *Chem. Phys. Lett.* **1999**, *313*, 63−68.

(7) Akimoto, S.; Takaichi, S.; Ogata, T.; Nishimura, Y.; Yamazaki, I.; Mimuro, M. *Chem. Phys. Lett.* **1996**, *260*, 147−152.

(8) Wasielewski, M. R.; Kispert, L. D. *Chem. Phys. Lett.* **1986**, *128*, 238−243.

(9) Cogdell, R. J.; Hipkins, M. F.; Macdonald, W.; Truscott, T. G. *Biochim. Biophys. Acta* **1981**, *634*, 191−202.

(10) van Grondelle, R.; Kramer, H. J. M.; Rijgersberg, C. P. *Biochim. Biophys. Acta* **1982**, *682*, 208−215.

(11) Angerhofer, A.; Bornhauser, F.; Gall, A.; Cogdell, R. J. *Chem. Phys.* **1995**, *194*, 259−274.

(12) Arnoux, B.; Ducruix, A.; Reisshusson, F.; Lutz, M.; Norris, J.; Schiffer, M.; Chang, C. H. *FEBS Lett.* **1989**, *258*, 47−50.

(13) Ermler, U.; Fritzsch, G.; Buchanan, S. K.; Michel, H. *Structure* **1994**, *2*, 925−936.

(14) McAuley, K. E.; Fyfe, P. K.; Ridge, J. P.; Cogdell, R. J.; Isaacs, N. W.; Jones, M. R. *Biochemistry* **2000**, *39*, 15032−15043.

(15) Cogdell, R. J.; Parson, W. W.; Kerr, M. *Biochim. Biophys. Acta* **1976**, *430*, 83−93.

(16) Lin, S.; Katilius, E.; Taguchi, A. K. W.; Woodbury, N. W. *J. Phys. Chem. B* **2003**, *107*, 14103.

(17) Frank, H. A.; Violette, C. A. *Biochim. Biophys. Acta* **1989**, *976*, 222−232.

(18) Frank, H. A.; Chynwat, V.; Hartwich, G.; Meyer, M.; Katheder, I.; Scheer, H. *Photosynth. Res.* **1993**, *37*, 193−203.

(19) Billsten, H. H.; Bhosale, P.; Yemelyanov, A.; Bernstein, P. S.; Polivka, T. *Photochem. Photobiol.* **2003**, *78*, 138−145.

(20) Polivka, T.; Zigmantas, D.; Herek, J. L.; He, Z.; Pascher, T.; Pullerits, T.; Cogdell, R. J.; Frank, H. A.; Sundstrom, V. *J. Phys. Chem. B* **2002**, *106*, 11016−11025.

(21) Frank, H. A.; Bautista, J. A.; Josue, J. S.; Young, A. J. *Biochemistry* **2000**, *39*, 2831−2837.

(22) Fujii, R.; Ishikawa, T.; Koyama, Y.; Taguchi, M.; Isobe, Y.; Nagae, H.; Watanabe, Y. *J. Phys. Chem. A* **2001**, *105*, 5348−5355.

(23) Andersson, P. O.; Bachilo, S. M.; Chen, R. L.; Gillbro, T. *J. Phys. Chem.* **1995**, *99*, 16199−16209.

(24) Frank, H. A.; Josue, J. S.; Bautista, J. A.; van der Hoef, I.; Jansen, F. J.; Lugtenburg, J.; Wiederrecht, G.; Christensen, R. L. *J. Phys. Chem. B* **2002**, *106*, 2083−2092.

(25) Papagiannakis, E.; Kennis, J. T. M.; van Stokkum, I. H. M.; Cogdell, R. J.; van Grondelle, R. *Proc. Natl. Acad. Sci. U.S.A.* **2002**, *99*, 6017−6022.

(26) Krueger, B. P.; Yom, J.; Walla, P. J.; Fleming G. R. *Chem. Phys. Lett.* **1999**, *310*, 57−64.

(27) Zhang, J.-P.; Fujii, R.; Qian, P.; Inaba, T.; Mizoguchi, T.; Koyama, Y.; Onaka, K.; Watanabe, Y.; Nagae, H. *J. Phys. Chem.* **2000**, *104*, 3683−3691.

(28) Walla, P. J.; Linden, P. A.; Hsu, C.-P.; Scholes, G. D.; Fleming, G. R. *Proc. Natl. Acad. Sci. U.S.A.* **2000**, *97*, 10808−10813.

(29) Polivka, T.; Pullerits, T.; Frank, H. A.; Cogdell, R. J.; Sundstrom, V. *J. Phys. Chem. B* **2004**, *108*, 15398−15407.

(30) Katilius, E.; Turanchik, T.; Lin, S.; Taguchi, A. K. W.; Woodbury, N. W. *J. Phys. Chem. B* **1999**, *103*, 7386-7389.

(31) Frank, H. A.; Taremi, S. S.; Knox, J. R. *J. Mol. Biol.* **1987**, *198*, 139−141.

(32) Frank, H. A.; Farhoosh, R.; Gebhard, R.; Lugtenburg, J.; Gosztola, D.; Wasielewski, M. R. *Chem. Phys. Lett.* **1993**, *207*, 88−92.

(33) Schenck, C. C.; Mathis, P.; Lutz, M. *Photochem. Photobiol.* **1984**, *39*, 407−417.

(34) Goldsmith, J. O.; Boxer, S. G. *Biochim. Biophys. Acta* **1996**, *1276*, 171−175.

(35) Takaichi, S. In *The Photochemistry of Carotenoids*; Frank, H. A., Young, A. J., Britton, G., Cogdell, R. J., Eds.; Advances in Photosynthesis Series; Kluwer Academic Publishers: Dordrecht, The Netherlands, 1999; pp 39−69.

(36) Zigmantas, D.; Hiller, R. G.; Sharples, F. P.; Frank, H. A.; Sundstrom, V.; Polivka, T. *Phys. Chem. Chem. Phys.* **2004**, *6*, 3009−3016.

(37) Frank, H. A.; Desamero, R. Z. B.; Chynwat, V.; Gebhard, R.; van der Hoef, I.; Jansen, F. J.; Lugtenburg, J.; Gosztola, D.; Wasielewski, M. R. *J. Phys. Chem. A* **1997**, *101* (2), 149−157.

(38) Macpherson, A. N.; Arellano, J. B.; Fraser, N. J.; Cogdell, R. J.; Gillbro, T. *Biophys. J.* **2001**, *80*, 923−930.

(39) Cerullo, G.; Polli, D.; Lanzani, G.; de Silvestri, S.; Hashimoto, H.; Cogdell, R. J. *Science* **2002**, *298*, 2395−2398.

(40) Zhang, J. P.; Skibsted, L. H.; Fujii, R.; Koyama, Y. *Photochem. Photobiol.* **2001**, *73*, 219−222.

(41) Mcdermott, G.; Prince, S. M.; Freer, A. A.; Hawthornthwaitelawless, A. M.; Papiz, M. Z.; Cogdell, R. J.; Isaacs, N. W. *Nature* **1995**, *374*, 517−521.

(42) Koepke, J.; Hu, X. C.; Muenke, C.; Schulten, K.; Michel, H. *Structure* **1996**, *4*, 581−597.

(43) Desamero, R. Z. B.; Chynwat, V.; van der Hoef, I.; Jansen, F. J.; Lugtenburg, J.; Gosztola, D.; Wasielewski, M. R.; Cua, A.; Bocian, D. F.; Frank, H. A. *J. Phys. Chem. B* **1998**, *102*, 8151−8162.

(44) Krueger, B. P.; Scholes, G. D.; Jimenez, R.; Fleming, G. R. *J. Phys. Chem. B* **1998**, *102*, 2284−2292.

(45) Papagiannakis, E.; Das, S. K.; Gall, A.; van Stokkum, I. H. M.; Robert, B.; van Grondelle, R.; Frank, H. A.; Kennis, J. T. M. *J. Phys. Chem. B* **2003**, *107*, 5642−5649.

(46) Walla, P. J.; Yom, J.; Krueger, B. P.; Fleming, G. R. *J. Phys. Chem. B* **2000**, *104*, 4799−4806.

(47) Zhang, J. P.; Inaba, T.; Watanabe, Y.; Koyama, Y. *Chem. Phys. Lett.* **2001**, *340*, 484−492.

(48) Fujii, R.; Onaka, K.; Kuki, M.; Koyama, Y.; Watanabe, Y. *Chem. Phys. Lett.* **1998**, *288*, 847−853.

(49) Sashima, T.; Shiba, M.; Hashimoto, H.; Nagae, H.; Koyama, Y. *Chem. Phys. Lett.* **1998**, *290*, 36−42.

(50) Polívka, T.; Zigmantas, D.; Frank, H. A.; Bautista, J. A.; Herek, J. L.; Koyama, Y.; Fujii, R.; Sundström, V. *J. Phys. Chem. B* **2001**, *105*, 1072−1080.

(51) Lin, S.; Taguchi, A. K. W.; Woodbury, N. W. *J. Phys. Chem.* **1996**, *100*, 17067−17078.

(52) Frank, H. A.; Bautista, J. A.; Josue, J.; Pendon, Z.; Hiller, R. G.; Sharples, F. P.; Gosztola, D.; Wasielewski, M. R. *J. Phys. Chem. B* **2000**, *104*, 4569−4577.

(53) Fujii, R.; Inaba, T.; Watanabe, Y.; Koyama, Y.; Zhang, J. P. *Chem. Phys. Lett.* **2003**, *369*, 165−172.

(54) King, B. A.; McAnaney, T. B.; deWinter, A.; Boxer, S. G. *J. Phys. Chem. B* **2000**, *104*, 8895−8902.

(55) Berera, R.; Herrero, C.; van Stokkum, L. H. M.; Vengris, M.; Kodis, G.; Palacios, R. E.; van Amerongen, H.; van Grondelle, R.; Gust, D.; Moore, T. A.; Moore, A. L.; Kennis, J. T. M. *Proc. Natl. Acad. Sci. U.S.A.* **2006**, *103*, 5343−5348.

(56) King, B. A.; de Winter, A.; McAnaney, T. B.; Boxer, S. G. *J. Phys. Chem. B* **2001**, *105*, 1856−1862.